Liquid Crystals
Publication details, including instructions for authors and subscription information:
http://www.informaworld.com/smpp/title~content=t713926090

Orientational order in nematic polymers - some variations on the Maier-Saupe theme

Stephen J. Picken[a]
[a] Nano Structured Materials, Department of Chemical Engineering, Delft University of Technology, Delft, The Netherlands

Online publication date: 06 July 2010

To cite this Article Picken, Stephen J.(2010) 'Orientational order in nematic polymers - some variations on the Maier-Saupe theme', Liquid Crystals, 37: 6, 977 — 985
To link to this Article: DOI: 10.1080/02678292.2010.488013
URL: http://dx.doi.org/10.1080/02678292.2010.488013

Liquid Crystals,
Vol. 37, Nos. 6–7, June–July 2010, 977–985

Taylor & Francis
Taylor & Francis Group

INVITED ARTICLE

Orientational order in nematic polymers – some variations on the Maier–Saupe theme

Stephen J. Picken*

Nano Structured Materials, Department of Chemical Engineering, Delft University of Technology, Delft, The Netherlands

(*Received 26 February 2010; accepted 15 April 2010*)

This review discusses some variations on the standard Maier–Saupe model which have been found to be useful for the understanding of main-chain and side-chain polymers. These models can be reduced to more general forms, providing a library of Maier–Saupe variants that may be applied to a wide range of thermotropic and lyotropic nematic liquid crystals and polymers. In addition, an adaptation of the Maier–Saupe model is proposed that includes a simplified excluded volume Onsager-like entropy term. This may allow a more quantitative evaluation of the importance of molecular shape on the temperature dependence of the $<P_2>$ orientational order parameter. Throughout this review some as yet unstudied problems are introduced that may provide the inspiration for further research.

Keywords: Maier–Saupe model, main-chain polymer, side-chain polymer

1. Introduction

This review discusses some variations on the standard Maier–Saupe model that have been found to be useful for the analysis of main-chain and side-chain polymers. These models can be reduced to more general forms that provide a library of Maier–Saupe variants that may be applied to a wide range of thermotropic and lyotropic nematic liquid crystals as well as liquid crystal polymers. First, we need to discuss the Maier–Saupe model in its basic form, and we note from the outset that it is somewhat irritating that, while the Maier–Saupe model is unusually successful, it is not at all clear why it actually works so well. We will return to this later.

In its most basic form the Maier–Saupe [1] model states that the tendency for a material to form a nematic phase is due to a molecular field potential resulting from the nematic continuum that interacts with a so-called test molecule (see Figure 1).

The molecular field nematic potential is assumed to have axial symmetry, resulting from the axial symmetry of the nematic phase, and is truncated to the first leading term of the general Legendre series expansion,

$$U = -\varepsilon <P_2> P_2(\cos\beta). \qquad (1)$$

The overall shape of the potential is described by $-P_2(\cos\beta) = -\frac{1}{2}(3\cos^2\beta - 1)$, which has minima at the north and the south pole ($\beta = 0$ and π). The strength of the potential depends on the pre-factor ε and the level of nematic order of the continuum as described by the $<P_2>$ orientational order parameter. This ensures that the nematic potential is switched off when the system is in the isotropic state, $<P_2> = 0$, and becomes stronger with increasing order of the environment. In a typical nematic phase $<P_2>$ varies with increasing temperature between about 0.8 and 0.4, although much higher values of $<P_2>$ may occur in main-chain polymer systems, up to about 0.95.

The pre-factor, ε, in Equation (1) is the strength of the potential and this allows adjustment of the model to the experimentally observed temperature, T_{NI}, the nematic–isotropic transition temperature. At this temperature the nematic phase transforms to the isotropic phase, exhibiting a (mildly) first-order phase transition with a relatively small latent heat, typically in the 0.5–1.5 J g^{-1} range.

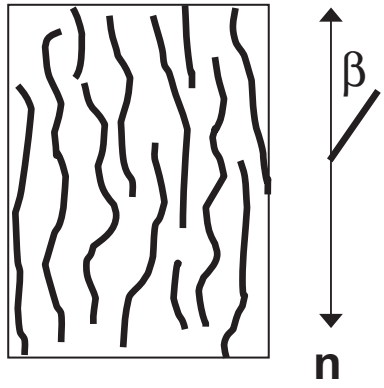

Figure 1. The local alignment of molecules in the nematic phase, the deviation angle β is the angle between the director **n** and the molecular long axis of the mesogens, or the molecular tangent vector in the case of main-chain polymers as depicted here.

*Email: s.j.picken@tudelft.nl

ISSN 0267-8292 print/ISSN 1366-5855 online

DOI: 10.1080/02678292.2010.488013
http://www.informaworld.com

Assuming the form of the potential in Equation (1) as a given, it is then straightforward to derive the orientational distribution function,

$$f(\beta) = \frac{1}{Z}\exp\left[\frac{\varepsilon}{k_B T} <P_2> P_2(\cos\beta)\right] \qquad (2a)$$

and

$$Z = \int_{-1}^{1} d\cos\beta \exp\left[\frac{\varepsilon}{k_B T} <P_2> P_2(\cos\beta)\right]. \qquad (2b)$$

Here Z is the partition function that ensures that $f(\beta)$ is normalised, i.e., the overall probability to find a particle is unity. The distribution function describes the probability to find a molecule at angle β with respect to the director.

The orientational distribution function can be used to derive the order parameter of the test molecule via a simple weighted average,

$$<P_2> = \frac{1}{Z}\int_{-1}^{1} d\cos(\beta).P_2(\cos\beta)\exp\left[\frac{\varepsilon}{k_B T} <P_2> P_2(\cos\beta)\right]. \quad (3)$$

Since the value of the order parameter of the test molecule has to be the same as that of the molecular field environment, Equation (3) provides an implicit relation between $<P_2>$ and k_BT/ε. Then, demanding that the actual state of the system should have the lowest free energy $F = <U> -T<S> \propto -½\varepsilon<P_2>^2 - k_BT \log Z$ leads to the result that for k_BT/ε larger than 0.22 we have an isotropic phase with $<P_2> = 0$, and below $k_BT/\varepsilon = 0.22$ we have a nematic phase with $<P_2> > 0$. This is shown in Figure 2.

It is remarkable that the Maier–Saupe model not only gives a qualitative interpretation of the essentials of thermotropic liquid crystals but that it also provides a good quantitative model for $<P_2>$ versus (T/T_{NI}). This is illustrated in Figure 3, showing some recent results for birefringence measurements on quinquephenyl (PPPPP) versus temperature which will be discussed in greater detail elsewhere [2]. It should be noted that quinquephenyl is considered to be an ideal model system to test the Maier–Saupe model due to its chemical (and conformational) simplicity [3]. The main challenge of quinquephenyl from an experimental point of view is its unusually high value of T_{NI} of about 425°C.

Despite its apparent success it is possible to discuss at length why the Maier–Saupe model works at all. That the potential strength scales with the order parameter of the environment is highly plausible, based on the fact that the Maier–Saupe potential can be derived

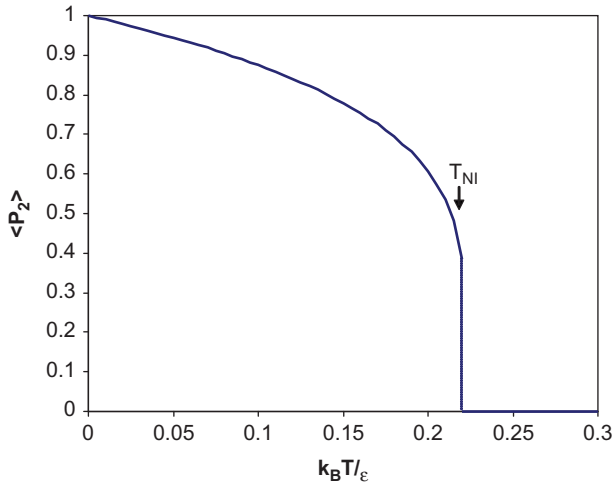

Figure 2. The scaled temperature dependence of $<P_2>$ as predicted by the Maier–Saupe model, by solving Equation (3) and minimising the free energy.

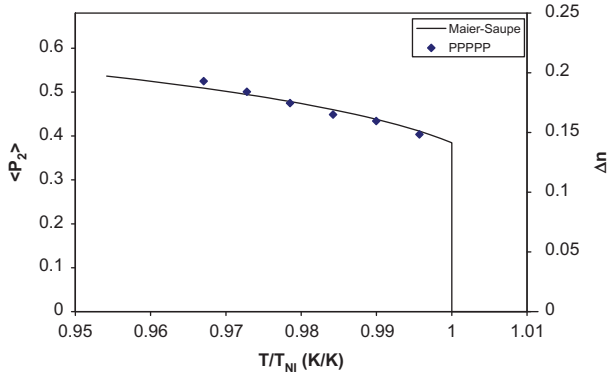

Figure 3. Birefringence and $<P_2>$ of quinquephenyl (PPPPP) versus T/T_{NI} compared to Maier–Saupe $<P_2>$ versus (T/T_{NI}), using $\Delta n = \Delta n_0 <P_2>$, with Δn_0 as an adjustable parameter.

by taking the average of all pair interactions. It also is relatively straightforward to include $<P_4>P_4(\cos\beta)$, $<P_6>P_6(\cos\beta)$ and higher terms to the potential [4]. However, this makes the model more difficult to compute, and moreover it does not really change the generic form. The P_2 truncation is sufficient if we wish to approach the problem in the linear elastic regime. The P_2 function gives a torque acting on the test molecule which is a linear function of the deviation angle, β, as it can be approximated as $P_2(\cos\beta) \approx 1 - \frac{3}{2}\beta^2$ via a Taylor expansion. This is analogous to the quadratic energy dependence of a linear elastic spring. In the desire to keep things as simple as possible, the potential as given by Equation (1) is the obvious choice. It is worth noting that using a more complicated form for U including P_4, P_6, etc., still yields a quadratic function

of the deviation angle β as, for instance, $P_4(\cos\beta) \approx 1–5\beta^2$ (β small), again giving rise to a linear torque versus the deviation angle.

The primary problem is the interpretation of the parameter, ε, in its original form; this was assumed to be related to the anisotropy of the molecular polarisability. Subsequent analysis showed that this interpretation did not provide a sensible value for the experimentally observed clearing temperatures, and additional suggestions were made. This is discussed, for instance, in the book by Chandrasekhar [5]. We can even adopt the approach that the potential, Equation (1), describes the Brownian motion of director fluctuations as proposed by Faber [6].

The present author believes that in the final analysis the primary physics of the Maier–Saupe model lies in the recognition that the effective potential acting on a particle has an axial symmetry, and that truncation of this potential to the leading P_2 term provides a simple and effective way to deal with the temperature dependence of the $<P_2>$ order parameter of nematic liquid crystals. In this simplified interpretation ε is viewed as an adjustable parameter. The primary strength of the Maier–Saupe model is its simplicity. It provides an excellent example of a generic molecular field model that has withstood the test of time.

Nevertheless, while aiming to retain the simplicity, I believe it is interesting to take the Maier–Saupe model further by introducing some variations that have been found to be useful when performing quantitative analysis of the temperature dependence of the $<P_2>$ order parameter. In particular such modification is found to be necessary when analysing main-chain and side-chain polymer nematic liquid crystals. Also, nematic side-chain polymers with non-linear optical (NLO) mesogenic groups (NLO-chromophores) have been studied for their field-induced polar and axial order. Introducing an external field into the Maier–Saupe potential appears to be useful as a method to model this, specifically in relation to the order parameter dynamics in AC electric fields [7]. Finally, I will introduce a variant of the Maier–Saupe model that contains an Onsager-like excluded volume entropy term. I believe this to be worthy of further analysis, and it may provide a starting point for a more quantitative assessment of the importance of molecular shape in thermotropic liquid crystals.

2. Variations of the Maier–Saupe model for main-chain and side-chain polymers

In the case of polymer liquid crystals it has been found useful to introduce two variants of the Maier–Saupe model. The first of these, sometimes described as the extended Maier–Saupe model (EMS), can be used for main-chain and side-chain liquid crystal polymers (LCPs) to describe the phase diagram and the temperature dependence of the $<P_2>$ order parameter [8, 9]. This model has been found to be of value as a method of taking into account the effect of coupling of the mesogenic groups, via the spacers and the polymer backbone with side chain LCPs (SCLCPs) and via the polymer chain itself for main chain LCPs (MCLCPs). Other chemically coupled systems to be considered could include dimers, dendrimers, etc.

The second model, introduced by myself and Van der Vorst and sometimes therefore referred to as the MSVP model, attempts to describe the effect of static external electric fields on the axial and polar order parameters [10]. This is useful in particular for non-linear optical SCLCPs that allow the poled nematic state to be frozen in by cooling below the glass transition temperature in the presence of the external field. During the preparation of this review it has become apparent in fact that the EMS and the MSVP models could (or should) have been merged to provide further generalisation.

2.1 *EMS model for main-chain LCP solutions*

Let us first sketch the essential ingredients of the EMS model in its original form. The primary step is the recognition that for nematic solutions of main-chain polymers the strength of the potential will scale with the concentration of polymer to some power and that the polymer chains themselves will have a temperature-dependent stiffness leading to a relative enhancement of the strength of the nematic potential as the temperature decreases. To achieve this it has been proposed [8, 9] that the strength of the potential, ε, may be written as

$$\varepsilon = \varepsilon^* c^2 L^2(T), \tag{5}$$

where c is the polymer concentration and $L(T)$ is the temperature-dependent contour projection length, given by

$$L(T) = L_p \frac{T_p}{T}\left[1 - \exp\left(-\frac{L_c T}{L_p T_p}\right)\right]. \tag{6}$$

The anisometry of the polymer chain at low molar mass and/or low temperature is governed by the physical length of the backbone, i.e. the contour length, L_c, which can be determined from the molar mass (e.g. the mass averaged molar mass, M_w) and the structure of the polymer repeat unit. This is the rigid-rod limit. On the other hand, for high molar mass and/or sufficiently high temperature the effective aspect ratio will be governed by the local stiffness of the polymer chain or Gaussian coil,

as described by the temperature-dependent persistence length, $L_p(T)$. The persistence length of a semi-flexible polymer chain is the correlation length of the orientation of the tangent vectors along the backbone, via $<\cos\theta>(s) = \mathbf{u_0}\cdot\mathbf{u_s} = \exp(-s/L_p)$, where s is the distance between the tangent vectors along the polymer contour. The persistence length, L_p, is thus a measure of the stiffness of the molecule.

The length of the contour projection (see Equation 6) reduces to the contour length, L_c, at low temperature and/or low L_c (M_w) – this is the rigid-rod limit, as can be readily verified. At high temperature and high L_c (M_w), Equation (6) reduces to the temperature-dependent persistence length $L_p(T) = L_p \,.\, T_p/T$. In many situations it is sufficient to simplify $L(T)$ to this high temperature, high L_c approximation. The constants L_p and T_p refer to the standard value of the persistence length which is usually determined at T_p = room temperature by studying dilute isotropic polymer solutions using viscosity measurements, static and dynamic light scattering, etc.

The exponent for the c-dependence in Equation (5) is motivated by the assumption that the interaction of the polymer chains is Van der Waals in nature ($1/r^6 \propto 1/V^2 \propto c^2$). This c^2 dependence is in agreement with the original form proposed by Maier and Saupe. Concerning the $L^2(T)$ dependence of ε, this is motivated by the fact that the Maier–Saupe potential derives from an average two-particle interaction.

The modification of the Maier–Saupe model shown in Equation (5) carries a number of implications. Firstly, it is possible to determine the dependence of T_{NI} on polymer concentration, as discussed later. Secondly, the temperature-dependent chain stiffness will act as a feedback loop, modifying the shape of the temperature dependence of $<P_2>$. This is demonstrated for the aramid polymer poly (4, 4'-benzanalidyleneterephthalamide) (DABT), (see Figure 4). Figure 5 shows the birefringence of a nematic 10.8% (w/w) solution of DABT in 99.8% H_2SO_4. In Figure 5 the birefringence has been converted to the anisotropy of the dielectric constant at optical frequencies, $\Delta\varepsilon = n_{//}^2 - n_{\perp}^2$, which is proportional to $<P_2>$. In practice the difference with the more commonly used relation $\Delta n = \Delta n_0 <P_2>$ is rather small, since they are roughly proportional: $\Delta\varepsilon = n_{//}^2 - n_{\perp}^2 = (n_{//} + n_{\perp})(n_{//} - n_{\perp}) \approx 2\bar{n}\Delta n$.

The concentration dependence of T_{NI} for a high molar mass sample is easily derived if it is assumed that $T_{NI} = Kc^{\alpha}$, which is not unreasonable as we would expect, *a priori*, that $T_{NI} = 0$ at zero liquid crystal polymer concentration. Using simple scaling relations we then find

$$T_{NI} \propto c^{\alpha} \propto \varepsilon \propto c^2 L^2 \propto c^2 T_{NI}^{-2} \propto c^{2-2\alpha}. \qquad (7)$$

This implies that $\alpha = 2 - 2\alpha$, or $\alpha = 2/3$. This is in remarkably good agreement with the experimental data, for example that found for DABT in H_2SO_4, see Figure 6. Inclusion of the full expression for $L(T)$ allows the prediction of the effect of polymer molar mass, which is also captured quite well. Note that to fit all of the experimental data requires the setting of only one adjustable parameter, ε*, in Equation (5).

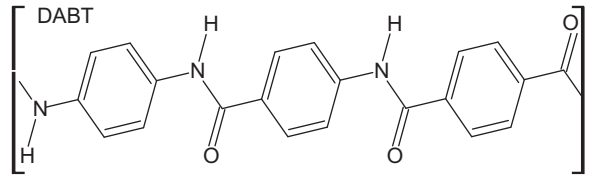

Figure 4. Structure of the main-chain aramid liquid crystal polymer DABT. This forms nematic solutions in H_2SO_4 (99.8%) between about 8–20% (w/w) polymer concentration.

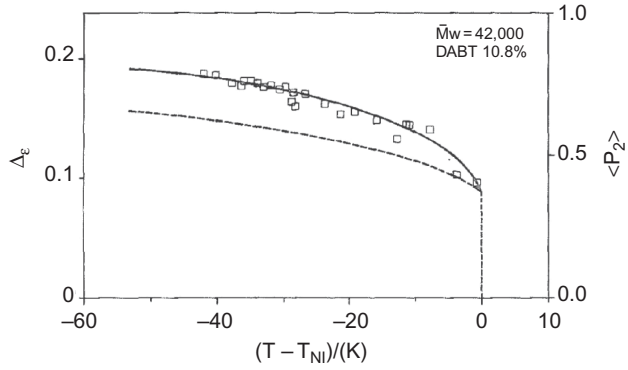

Figure 5. The anisotropy of the dielectric constant of DABT versus temperature for a polymer sample in a 10.8% (w/w) solution in H_2SO_4 (99.8%), with a weight-averaged molar mass, M_w, of 42 000, from [9], with permission.

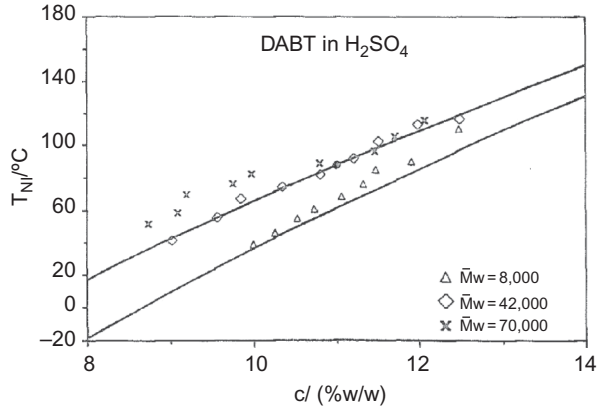

Figure 6. Nematic–isotropic transition temperatures of DABT in H_2SO_4, taken at the 50% N–I phase separation point, versus polymer concentration, for three molar mass values, as indicated. The filled point is used to determine ε* in Equation (5). Taken from [8], with permission.

The reasonably successful description of both $<P_2>$ versus (T/T_{NI}) and $T_{NI}(c)$ for aramid solutions provides further support for the exponents used in Equation (5) for the effects of stiffness and concentration. The EMS model as first used for aramid polymers has been found to be applicable for other main-chain polymer systems such as cellulose in phosphoric acid [11], and poly(2, 6-diimidazo [4, 5-b: 4', 5' -e] pyridinylene -1, 4- (2, 5- dihydroxy)phenylene) (PIPD) in polyphosphoric acid [12].

2.2 *Generalised forms*

If we examine the EMS model described by Equations (1) and (5) for the high molecular weight limit, it is apparent that the temperature dependence of the standard Maier–Saupe model, ε/k_BT, is replaced by a new temperature dependence, C/T^3, as Equation (5) implies that the strength of the potential itself scales as $1/T^2$,

$$U \propto \varepsilon T^{-1} \propto L^2(T)T^{-1} \propto T^{-2}T^{-1} \propto T^{-3}. \quad (8)$$

The standard Maier–Saupe model depends on the dimensionless parameter, T/T_{NI}. In the EMS model, which works quite well for aramid solutions and other main-chain polymers, the value of T/T_{NI} is effectively replaced by $(T/T_{NI})^3$. Based on this, an obvious generalisation of the Maier–Saupe model is to replace T/T_{NI} by $(T/T_{NI})^\alpha$, where $\alpha = 1$ corresponds to the standard Maier–Saupe model and $\alpha = 3$ is applicable to main-chain polymer solutions. Other values of α may occur and could provide further clues on subtle interactions occurring in the system. For instance, loosely coupled side-chain LCPs seem to be described by fitting $<P_2>$ versus (T) with $\alpha = 1$ (standard Maier–Saupe), whereas more tightly coupled systems seem to require higher values for α in the region of 2–3. This suggests that the anomalous temperature dependence of $<P_2>$ for the tightly coupled mesogens is induced by the coupling of the mesogens via the backbone and spacers, involving a temperature-dependent stiffness of the coupling coefficient. This implies introducing a variant of the EMS model for thermotropic side-chain polymers of the form

$$U = -\varepsilon\left(\frac{T_{NI}}{T}\right)^{\alpha-1} <P_2> P_2(\cos\beta). \quad (9)$$

Applying this changes the standard Maier–Saupe evaluation of $<P_2>$ versus (T/T_{NI}) into $<P_2>$ versus $((T/T_{NI})^\alpha)$, and calculating the EMS model therefore only involves a simple remapping of the temperature scale. For practical calculations it is sufficient to use an approximate expression for the EMS temperature dependence of $<P_2>$ for $T \le T_{NI}$, and $<P_2> = 0$ for $T > T_{NI}$:

$$<P_2> = 0.1 + 0.9\left[1 - 0.99\left(\frac{T}{T_{NI}}\right)^\alpha\right]^{\frac{1}{4}}. \quad (10)$$

This form was determined by optimising the analytical approximation to the numerically calculated Maier–Saupe curve (with $\alpha = 1$) by trial and error, and is correct to within about 1%. Other values of α then allow convenient calculation of the extended Maier–Saupe curve, $<P_2>$ versus $(T/T_{NI})^\alpha$.

As an example of the application of the EMS model to a complex nematic system, this is illustrated later for the equimolar charge-transfer complex of 11-[pentakis(4-methoxyphenylethynyl)phenoxy]-undecan-1-ol (**D1**) and poly[11-((Z,E)-2,4,7-trinitro-9-fluorenylideneaminooxy)-undecyl acrylate-co-methyl acrylate] (**PA1**), (see Figure 7, which exhibits a N_L to N_D nematic–nematic phase transition). Figure 8 shows the temperature dependence of $<P_2>$ for this system, which requires $\alpha = 2$ and $\alpha = 1$ for the N_L and the N_D phase, respectively (see [13] for further details).

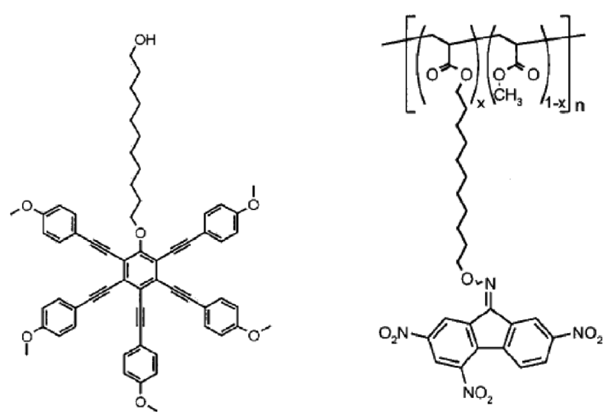

Figure 7. Structure of **D1** and **PA1**.

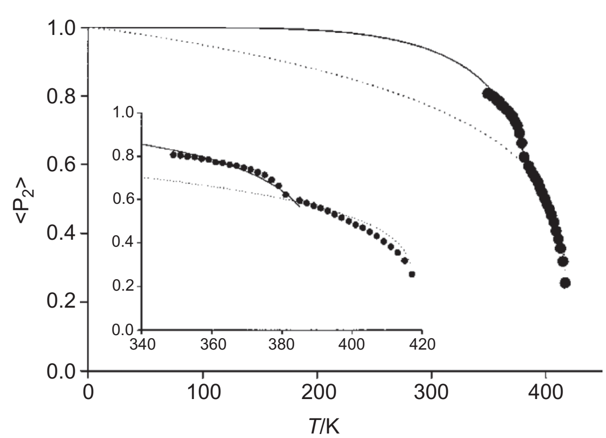

Figure 8. Temperature dependence of the orientational order parameter of the equimolar charge-transfer complex of **D1** and **PA1**: (•) experimental data; (. . ..) and (—) fits of the N_L phase and N_D phase using $\alpha = 2$ and $\alpha = 1$, respectively. The inset shows a magnification. Taken from [13], with permission.

Finally, it is intriguing to note that in the EMS model the remapping of the temperature scale is analogous to the remapping of the time scale, as occurs in the widely used Kohlraush stretched exponential expression for glass dynamics [14]: $\Delta\phi(t) = \Delta\phi_0 \exp(-(t/\tau)^{\beta})$. This may provide clues for a more rigorous derivation of the form proposed in Equation (9).

2.3 A Maier–Saupe-like model for field-induced order parameters of side-chain LCPs

Side-chain LCPs have been studied for applications in NLO devices making use of field-induced polar order of the mesogenic chromophores. In the absence of an external electric field the nematic phase has uniaxial symmetry without polar order, i.e. only the even orientational order parameters $<P_2>$, $<P_4>$, etc., are non-zero. On application of an external poling field the $<P_1> = <\cos\beta>$ and $<P_3> = <\frac{1}{2}(5\cos^3\beta - 3\cos\beta)>$ order parameters are also non-zero and we obtain field-induced polar order in the system. The question becomes: what effect does the axial order of the nematic phase have on the level of polar order at a given electric field strength?

To describe this it is relatively straightforward to include electric field-dependent terms into the Maier–Saupe potential [10], as in

$$U = -\varepsilon < P_2 > P_2(\cos\beta) - \mu_0 E \cos\beta - \tfrac{1}{3}\Delta\alpha E^2 P_2(\cos\beta). \quad (11)$$

The first field-dependent term describes the interaction with the permanent dipole moment, μ_0, of the chromophore. The second field-dependent term, which can usually be neglected, describes the effect of the field-induced dipole moment, where $\Delta\alpha$ is the anisotropy of the molecular polarisability, $\Delta\alpha = \alpha_{//} - \alpha_{\perp}$. In the absence of a nematic phase the field-dependent terms will cause a certain level of polar and axial alignment in the system, and when the system becomes nematic the electric field will further enhance $<P_2>$ and the field dependence of the polar order will become larger.

The effect of axial order on the polar order can be calculated analytically by comparing the Ising model, with $<P_2> = 1$ in the absence of a field, and the isotropic model using $U = -\mu_o E \cos\beta$, i.e. initially with $<P_2> = 0$. For the Ising model it is found that

$$<\cos^3\beta>_{\text{Ising}} \approx \frac{\mu_0 E}{k_B T} \quad (12)$$

and for the isotropic model

$$<\cos^3\beta>_{\text{Isotropic}} \approx \frac{\mu_0 E}{5 k_B T}, \quad (13a)$$

$$<P_2>_{\text{Isotropic}} \approx \frac{1}{15}\left(\frac{\mu_0 E}{k_B T}\right)^2. \quad (13b)$$

These expressions are valid for small field strength in the linear regime; the full expressions, including the non-linear response at high fields, are given in the paper by Van der Vorst and Picken [10].

From this simplified analysis it is observed that perfect axial order leads to a five-fold enhancement of $<\cos^3\beta>$ compared to an initially isotropic sample. In a typical nematic phase the $<P_2>$ value is smaller, giving rise to a somewhat smaller enhancement factor, typically about 3–4, which has subsequently been verified experimentally. The average value of $<\cos^3\beta>$ is a useful quantity as it is directly related to the experimentally determined linear electro-optic, or Pockels, effect via $\chi^{(2)}_{ZZZ} = NF\beta_{ZZZ}\langle\cos^3\beta\rangle$, where β_{ZZZ} is the ZZZ component of the molecular hyperpolarisability, N is the number density and F is the local-field correction. It is straightforward to verify that $<\cos^3\beta> = (3<P_1> + 2<P_3>)/5$. Figure 9 shows the field-induced polar order predicted by this model and some comparisons with simplified approximations.

It is also worth noting that this model predicts that above a certain field strength the $<P_2>$ versus temperature curves become continuous, i.e. the field-dependent phase diagram exhibits a critical point, as shown in Figure 10.

The model described by Equation (11) is in fact the type of model which might be proposed for a nematic liquid crystal of low molar mass with NLO mesogenic

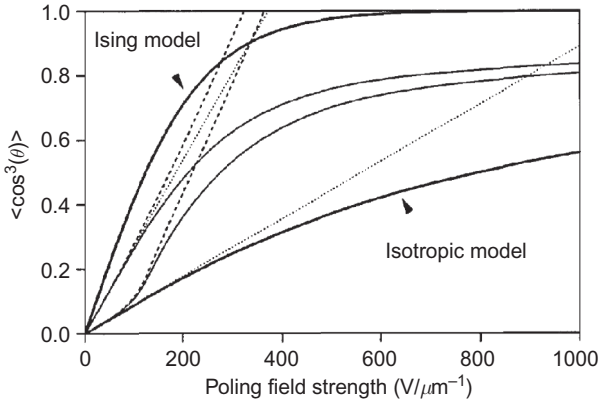

Figure 9. The polar order $<\cos^3(\beta)>$ calculated as a function of the applied electric field, assuming 7 D for the molecular dipole moment, and 47 Å^3 for the anisotropy of the molecular polarisability. The thick curves are the exact solution of the Ising and isotropic models, the thin solid curves are obtained using the potential as given in Equation (11), for an initially isotropic and an initially nematic zero-field state. The dotted and dashed lines are from a linear approximation of the so-called SKS model [15]. Taken from Figure from [10], with permission.

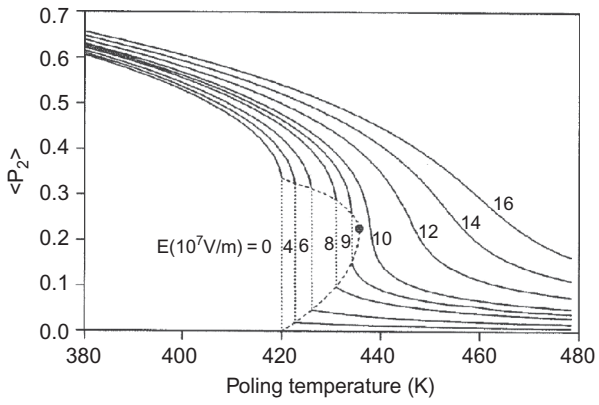

Figure 10. The variation of the $<P_2>$ order parameter with variation in the poling temperature for the values of the molecular dipole moment, and anisotropy of the molecular polarisability, as in Figure 9. Note the critical point between $E = 9 \times 10^7$ and 10×10^7 V/m. Taken from [10], with permission.

groups, such as an alkyl nitrostilbene or similar structure. The question arises as to whether the standard Maier–Saupe model is applicable to a side-chain LCP (in the absence of a field). In the event, some side-chain LCPs do indeed require a steeper $<P_2>$ dependence, as discussed earlier, see Figure 8. Based on this observation an obvious further generalisation of the model would be to introduce a temperature-dependent strength of the nematic potential, using the form proposed in Equation (9),

$$U = -\varepsilon\left(\frac{T_{NI}}{T}\right)^{\alpha-1} <P_2> P_2(\cos\beta) - \mu_0 E \cos\beta - \tfrac{1}{3}\Delta\alpha E^2 P_2(\cos\beta). \quad (14)$$

While this approach may be useful, it is not immediately obvious how to calculate the temperature-dependence of the various (field-induced) order parameters in a straightforward manner. After dividing U by k_BT the first term will give a $(1/T)^{\alpha}$ dependence, while the other terms retain the standard $1/T$ dependence. Solving Equation (13) is no longer a simple remapping procedure.

2.4 Extending the Maier–Saupe model with a non-thermal Onsager-like term

As a final variant of the Maier–Saupe model I would like to introduce the form of the nematic potential

$$U = -(\varepsilon_1 + \varepsilon_2 T) <P_2> P_2(\cos\beta). \quad (15)$$

The ε_1 term is the regular Maier–Saupe potential, whereas the $\varepsilon_2 T$ term may be recognised as an entropy, as it is proportional to T. Applying Equation (15) into a Bolzmann factor introduces the variable, U/k_BT, so that the ε_1 term gives a temperature dependence and the ε_2 term provides a non-thermal contribution, since the temperature divides out. If we consider this non-thermal part only (setting $\varepsilon_1 = 0$) we obtain

$$U = -\varepsilon_2 T <P_2> P_2(\cos\beta) \quad (16)$$

which is analogous to the two-particle excluded volume (entropy) term in the Onsager model [16]. For rods with L/D aspect ratio,

$$U = 2kTDL^2|\sin\gamma|. \quad (17)$$

It is worth stressing that the Onsager model is derived by considering the two-particle excluded volume only, which is probably acceptable for high aspect ratio rigid rods. If we have a high concentration of hard rods of lower aspect ratio the problem of excluded volume becomes intractable. Attempts to calculate general expressions for the three-particle excluded volume have been unsuccessful, and higher order terms would be required. The form proposed in Equation (16) (and (15)) is therefore a postulated first-order approximation for this excluded volume entropy. It has the required up / down symmetry, is a quadratic function of the deviation angle, and through inclusion of temperature it provides a non-thermal entropy response by the system. In effect it is an excluded volume term, strongly reminiscent of the original Maier–Saupe model.

Predicting the phase diagram resulting from Equation (15) is straightforward if we introduce a fictive temperature, T_f, according to

$$\frac{(\varepsilon_1 + \varepsilon_2 T)}{k_B T} = \frac{\varepsilon}{k_B T_f} \quad (18)$$

and solving for T_f gives

$$T_f = \frac{\frac{\varepsilon}{\varepsilon_1} T}{1 + \frac{\varepsilon_2}{\varepsilon_1} T} = \frac{\alpha T}{1 + \beta T}. \quad (19)$$

In particular, by simple rearrangement we also obtain

$$T_{NI} = \frac{T_{f,NI}}{\alpha - \beta T_{f,NI}}. \quad (20)$$

Expressions (19) and (20) can be used to remap the real temperature to the fictive temperature, which can then be used to calculate the corresponding order parameter, $<P_2>$, using Equation (10). It should be noted that T_{NI} may become infinite if the non-thermal contribution $\varepsilon_2 T$ dominates, and the final expression for the temperature remapping procedure is given as

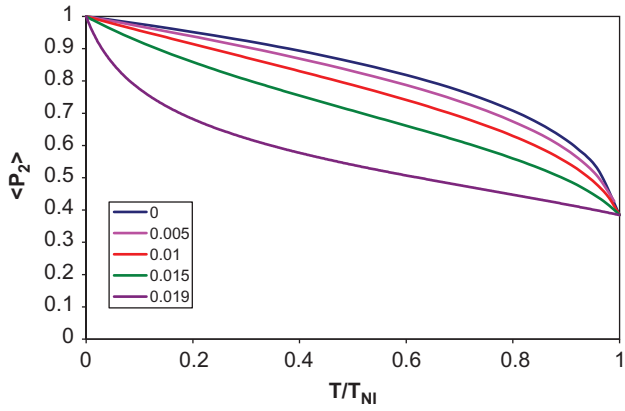

Figure 11. The temperature dependence of the $<P_2>$ order parameter predicted using the potential as proposed in Equation (14). The curves are generated using $\alpha = 1$ and β as indicated in the Figure using the remapping procedure as described by Equation (18). The value of $T_{f,NI}$ was arbitrarily set at 50 K (color version online).

$$\frac{T}{T_{NI}} = \frac{T_f}{T_{f,NI}} \frac{\alpha - \beta T_{f,NI} \frac{T_f}{T_{f,NI}}}{\alpha - \beta T_{f,NI}}. \qquad (21)$$

It is interesting to examine some $<P_2>$ curves for a few selected values of these parameters, (see Figure 11). The results are shown for systems that still have a nematic–isotropic temperature at finite T_{NI}, and in which the x-axis is the reduced temperature, T/T_{NI}. From Figure 11 it becomes clear that by introducing a non-thermal term in the Maier–Saupe potential the $<P_2>$ temperature dependence can change in a qualitative sense. The temperature dependence changes close to T_{NI} from the usual convex shape to become almost linear. In addition, for certain values of the parameters the curve contains both convex and concave regions. It would be interesting to compare this model with experimental data for $<P_2>$, especially for systems with a systematic variation in shape, for example biphenyls, terphenyls, tetraphenyls, and so on. It could also be useful to study the $<P_2>$ temperature dependence at elevated pressure, as it would seem reasonable to expect molecular shape and excluded volume to become more important as the pressure is increased. Of course the model may also be relevant in analysing the actual location of T_{NI} versus molecular shape.

3. Summary and conclusions

A range of variants of the Maier–Saupe model that have been found useful for describing the phase behaviour and temperature-dependence of the order parameters for a variety of main-chain and side-chain liquid crystal polymers have been discussed. These models include methods of dealing with the effect of mesogen and polymer concentration. In addition they explain, at least partly, the steeper temperature dependence of orientational order often observed around T_{NI}. In some cases, for instance for side-chain polymers with NLO-mesogens, it has also been found useful to include the effect of static external electric fields, giving rise to field-induced polar order parameters. The degree of polar order is found to be coupled to the axial order and this rather complex situation can be dealt with quite successfully by including electric field-dependent terms in the Maier–Saupe potential. Finally, we have introduced the field-dependent extended Maier–Saupe model, and also a Maier–Saupe model containing a non-thermal excluded volume entropy term, somewhat analogous to the Onsager model. We expect that these Maier–Saupe variants may find useful application in the improved analysis of the order parameter, for both molecular and polymeric nematic liquid crystals. It should be noted that others have made excellent contributions to the theory of side-chain and main-chain LCPs based on the original ideas of Maier and Saupe, notably in papers by Warner and co-workers [17, 18].

Acknowledgements

I wish to acknowledge the large number of past and present colleagues who have contributed to this work.

References

[1] Maier, W.; Saupe, A. *Z. Naturforsch.* **1958**, *13a*, 564–566; Maier, W.; Saupe, A. *Z. Naturforsch.* **1959**, *14a*, 882–889; Maier, W.; Saupe, A. *Z. Naturforsch.* **1960**, *15a*, 287–292.
[2] Kuiper, S.; Norder, B.; Jager, W.F.; Dingemans, T.J.; Picken, S.J. To be submitted for publication.
[3] Dingemans, T.J.; Madsen, L.A.; Zafiropoulos, N.A.; Lin, W.B.; Samulski, E.T. *Phil. Trans. A, Math. Phys. Eng. Sci.* **2006**, *364*, 2681–2696.
[4] Humphries, R.L.; James, P.G.; Luckhurst, G.R. *J. Chem. Soc., Faraday Trans. II.* **1972**, *68*, 1031–1044.
[5] Chandrasekhar, S. *Liquid Crystals*; Cambridge University Press: Cambridge, 1992.
[6] Faber, E. *Proc. Roy. Soc. A* **1977**, *353*(*1673*), 247–259.
[7] Picken, S.J. *Macromol. Symp*. **2000**, *154*, 95–104.
[8] Picken, S.J. *Macromol*. **1989**, *22*, 1766–71.
[9] Picken, S.J. *Macromol*. **1990**, *23*, 464–70.
[10] Van der Vorst, C.P.J.M.; Picken, S.J. *J. Opt. Soc. Am. B.* **1990**, *7*, 320–325.
[11] Boerstoel, H.; Maatman, H.; Picken, S.J.; Remmers, R.; Westerink, J.B. *Polymer* **2001**, *42*, 7363–7369.
[12] Picken, S.J.; Boerstoel, H.; Northolt, M.G. In *The Encyclopedia of Materials: Science and Technology:* Buschow, K.H.J., Cahn, R., Flemings, M.C., Ilschner, B., Kramer, E.J., Mahajan, S., Veyssiere, P., Eds.; Elsevier: Oxford, 2001; pp 7883–7887.

[13] Kouwer, P.H.J.; Jager, W.F.; Mijs, W.J.; Picken, S.J. *Macromol.* **2002**, *35*, 4322–4329.
[14] Kohlrausch, R. *Annalen der Physik and Chemie (Poggendorff)* **1854**, *91*, 179.
[15] Singer, K.D.; Kuzyk, M.G.; Sohn, J.E. *J. Opt. Soc. Am. B* **1997**, *4*, 968–976.
[16] Onsager, L. *Annals. of the New York Academy of Sciences.* **1949**, *51*(*4*), 627–659.
[17] Warner, M. *Mol. Cryst. Liq. Cryst.* **1988**, *155*, 433–442.
[18] Wang, X.J.; Warner, M. *J. Phys. A: Math. Gen.* **1986**, *19*, 2215–2227.